

Modification of the Properties and Sulfur Resistance of a Pd/SiO₂ Catalyst by La Addition

N. S. Fígoli,* P. C. L'Argentiere,* A. Arcoya,† and X. L. Seoane†¹

**Instituto de Investigaciones en Catálisis y Petroquímica INCAPE (UNL, FIQ-CONICET), Santiago del Estero 2654, 3000 Santa Fe, Argentina; and †Instituto de Catálisis y Petroquímica, CSIC, Campus Universidad Autónoma, Cantoblanco, 28049 Madrid, Spain*

Received June 9, 1994; revised February 9, 1995

The effect of LaCl₃ on the properties and deactivation of Pd/SiO₂ catalysts by thiophene poisoning in the hydrogenation of ethylbenzene has been studied. Gas chemisorption and TPR measurements, respectively, show that Pd dispersion increases with the ratio La/Pd and that La hinders palladium reduction. The presence of Pdⁿ⁺ species on Pd/SiO₂ was evidenced by XPS, but the incorporation of lanthanum decreases the concentration of Pdⁿ⁺. Deactivation results show that La improves the Pd sulfur resistance, which goes through a maximum for the catalyst with La/Pd = 2 atomic ratio. This effect cannot be attributed to the increase in Pd dispersion produced by La, a decorating effect of Pd by La species, or sulfur adsorption by La. From the mechanism for metal poisoning by thiophene at 493 K, which involves the hydrogenolysis of the sulfur compound on the metal sites, an alternative explanation of the results is suggested. It seems that LaCl₃ essentially plays a diluent role, disrupting the ensembles of palladium atoms required for the breaking of the C–S bond. XPS and TPR results, which indicate the occurrence of a weak Pd–La interaction, support this hypothesis. Thus, the catalysts containing lanthanum are more sulfur resistant, with a maximum for La/Pd = 2. For this sample, XPS suggests that a slight charge transfer from Pd to La takes place and therefore the electronic effect of Pdⁿ⁺ is added to the geometric effect produced by La³⁺. © 1995

Academic Press, Inc.

INTRODUCTION

Palladium-based catalysts have been proven to be highly active and selective in several important commercial reactions, including automotive pollution control, synthesis of methanol from CO + H₂, and hydrocarbon hydrogenation. A very comprehensive review of the physicochemical properties and catalytic behaviour of both metallic and electron-deficient palladium has been recently published (1).

In the last years, it has been well established that when lanthana is used as a support or when it is added to palladium or rhodium catalysts, it improves their performance

mainly in methanol production (2–6). Lanthana itself is inactive for this reaction. Several hypotheses have been put forward to explain the promoter effect of lanthanum oxide. According to various authors (7, 8), during thermal treatments, the metal particles are decorated by LaO_x moieties ($x < 1.5$), creating a Pd–LaO_x interface in a SMSI state, which exhibits a high catalytic activity for CO hydrogenation. In this case, a transfer of the excess charge of La to Pd particles has been observed by XPS, giving a Pd more electronegative than Pd⁰ (9). In other cases, it was found that the interaction of La₂O₃ and palladium precursors creates and stabilizes electron-deficient species (Pdⁿ⁺), which are essential for the production of methanol (10). The majority of these works deal with the influence of lanthana in methanol synthesis and only a few are concerned with the effect of LaCl₃ (8). But, to our knowledge, less attention has been devoted to the effect of lanthanum on the catalytic properties of palladium in hydrocarbon hydrogenation reactions.

One of the major problems with palladium is the high sensitivity to sulfur compounds usually present in hydrogenation feedstocks (11). Well-documented reviews devoted to the effect of sulfur on metal catalysts are available in the literature (12, 13). Because of the commercial and fundamental scientific interest of this subject, it is important to have better insight into the phenomena of palladium deactivation by sulfur poisoning. In a previous paper (14) it was reported that there is a positive correlation between the concentration of electron-deficient Pdⁿ⁺ species and the sulfur resistance of the catalysts. Such species were formed when catalysts were prepared from PdCl₂ acid solutions and reduced at temperatures below 723 K. The purpose of this work is to study the modifications produced by lanthanum on both the properties of Pd/SiO₂ catalyst and its resistance towards thiophene during ethylbenzene hydrogenation.

Fresh catalysts were characterized by temperature-programmed reduction (TPR), H₂ and CO chemisorption, X-ray diffraction (XRD), and X-ray photoelectron spectroscopy (XPS); and deactivated catalysts were character-

¹ To whom correspondence should be addressed.

ized by XPS, X-ray fluorescence, and gas chemisorption. Experimental results show that lanthanum modifies the dispersion and surface chemical state of palladium in addition to its sulfur resistance. We analyze here different hypotheses in order to explain the effect of lanthanum on sulfur resistance, including an approach based on a cooperative Pd–La local electronic interaction with an La geometric effect.

METHODS

Catalyst Preparation

Five catalysts containing 0.5 wt% Pd and La/Pd atomic ratios between 0 and 4.5, were prepared by the incipient wetness coimpregnation technique. Silica G-57 from W. R. Grace ($\text{SiO}_2 > 99.6$ wt%), with a BET surface area of $300 \text{ m}^2 \text{ g}^{-1}$, a pore volume of $1 \text{ cm}^3 \text{ g}^{-1}$, and particle size 0.8–1.41 mm, was used as support. The SiO_2 was calcined at 823 K before impregnation. Impregnating solutions were prepared by dissolving the desired amounts of PdCl_2 and La_2O_3 in the appropriate volume of a 1 M HCl solution; La_2O_3 was previously dehydrated at 773 K. In this way, PdCl_2 is transformed into H_2PdCl_4 , and La_2O_3 into $\text{LaCl}_3 \cdot n \text{ H}_2\text{O}$. This procedure was selected in order to get the same concentration of chloride ions in all the samples. After drying at 393 K overnight, precursors were calcined at 573 K for 4 h in an air stream. Prior to reaction, samples were reduced *in situ* at 573 K for 5 h in a hydrogen stream. The chemical composition of the catalysts is given in Table 1. Additionally, two samples containing 5 wt% $\text{LaCl}_3/\text{SiO}_2$ without calcining (sample F) and calcined (sample G) were also prepared following the same procedure.

Catalyst Characterization

Catalyst reducibility was determined by the temperature-programmed reduction technique. TPR experiments were performed in a flow system with a thermal conductivity detector. Samples of 0.5 g of the calcined precursors were outgassed at 573 K for 1 h in an Ar stream and then

cooled to 273 K. TPR profiles were registered by heating the samples from 273 K to 773 K, at 6 K min^{-1} , in a gas flow rate of 5% H_2/Ar (30 ml min^{-1}).

Catalyst dispersion was determined from two different techniques.

(i) Hydrogen chemisorption was performed by the hydrogen back-sorption method (5) using a volumetric adsorption system at room temperature with the following steps: (a) outgassing the sample at 573 K for 30 min; (b) reduction in flowing H_2 (30 ml min^{-1}) at 573 K for 5 h; (c) outgassing at 573 K for 60 min; (d) measurement of H_2 uptake at room temperature; (e) outgassing at room temperature for 30 min; (f) measurement of H_2 uptake at room temperature; (g) outgassing at room temperature for 30 min; and (h) dead volume determination.

The first H_2 uptake (step (d)) corresponds to both adsorbed and absorbed hydrogen. During outgassing at room temperature, only absorbed hydrogen is eliminated (15). During step (f) the hydrogen uptake corresponds to adsorbed hydrogen. An $\text{H}_{\text{ads}}/\text{Pd}_s$ stoichiometry of 1/1 was used.

(ii) CO chemisorption was carried out following the technique described in (16) and using a $\text{CO}_{\text{ads}}/\text{Pd}_s$ stoichiometry of 1.15/1, as recommended by Farrauto (17).

Both methods were selected for comparative purposes. From the CO chemisorption data, the number of exposed palladium atoms (N_{Pd} in Table 5) used to determine the sulfur resistance parameters was calculated.

X-ray photoelectron analysis was carried out on a Shimadzu ESCA 750 Electron Spectrometer coupled to a Shimadzu ESCAPAC 760 Data System. Correction for binding energies due to sample charging was effected by taking the Si $2p_{1/2}$ line at 103.2 eV as an internal standard. The binding energy (BE) values of the Pd $3d_{5/2}$ and La $3d_{5/2}$ peaks maxima were used to follow the superficial chemical state of palladium and lanthanum. Determination of the surface atomic ratios was made by comparing the areas of the peaks after background subtraction and corrections due to differences in escape depths (18) and in photoionization cross sections, using Scofield's results (19). After reduction, the samples were introduced into

TABLE 1
Characterization of the Catalysts by TPR and Chemisorption of H_2 and CO

Catalyst	La/Pd (atomic ratio)	La (wt%)	TPR, T_{max} (K)	D (%) H_2	D (%) CO
A	0	0	367	12.0	11.0
B	1	0.65	376	15.0	14.0
C	2	1.30	393	20.0	18.0
D	3	1.95	399	24.0	21.2
E	4.5	2.93	403	21.0	20.0
G	—	1.30	—	0	0

the sample holder under isoctane and protected from exposure to air by a meniscus of this liquid. Isoctane was removed during pumping in the preparation chamber of the XPS equipment. This operating procedure ensures (20) that there is no modification of the electronic state of palladium and lanthanum. In order to confirm that air exposure is not a concern, a fraction of catalysts A–E were exposed, after being reduced, to the atmosphere for 1 h to 15 days. No modifications in the Pd and La BE were observed after those periods, thus indicating that there were no electronic modifications of Pd and La. Similar results have also been reported by other authors (21–23).

X-ray diffraction patterns were recorded with a Seifert C-3000 powder diffractometer, using CuK α radiation, at 40 kV and 40 mA, with slits of 1°, 0.1°. Before performing XRD patterns, samples were protected against hydration by keeping them in a desiccator.

Catalyst Deactivation Measurement

Hydrogenation of ethylbenzene was used to evaluate the stability of the catalysts towards sulfur. Experiments were carried out in a conventional pressure system (24), with a fixed-bed flow reactor containing 5 g of catalyst, diluted with SiC in order to get a more isothermal profile. A bed of SiC above the catalyst was employed as pre-heater. The reaction conditions were 2 MPa, 493 K, hydrogen to ethylbenzene molar ratio = 10, and liquid space velocity 10 h⁻¹. High-purity hydrogen was successively passed through a Deoxo purifier and a 5A molecular sieve filter. Ethylbenzene (RPE grade) was diluted 30/70 wt/wt with decalin (RPE grade) and the liquid feed was contaminated with 100 ppm of thiophene.

The reactor was heated to the reaction temperature under an adjusted hydrogen flow. When this temperature was reached, the liquid feed was introduced and the first sample was collected 10 min later (time = 0). To follow the activity decay as a function of time on stream, i.e., the thiophene fed, analyses of the effluent were performed each 3 min until the catalyst was completely deactivated.

Catalyst activity for ethylbenzene hydrogenation, in the absence of thiophene, was determined under the same experimental conditions used in the deactivation experiments and following analogous procedures to collect the first sample (at 10 min). Afterwards, samples were periodically collected in order to evaluate the catalyst stability. Each experiment was run for 10 h.

The reactor effluent was condensed at 273 K and analyzed by gas-liquid chromatography (TCD). Liquid samples were injected in a 4 m \times 3.18 mm o.d. column packed with 1,2,3-tris(2-cyanoethoxy)propane (10 wt%) on Chromosorb P (60–80 mesh), at 353 K. The exit gas stream was analyzed at 313 K in a 4 m \times 3.18 mm o.d. column

of powdered activated charcoal. Helium (40 cm³ min⁻¹) was used as carrier gas.

Following a conventional methodology (25), several experiments were performed in order to examine possible diffusional effects: (a) At constant F/W (10 h⁻¹) and H₂ to liquid hydrocarbon ratio but changing both the liquid flow and catalyst weight between 50/5 and 150/15. The conversion remained constant. (b) Using different catalyst particle sizes, between 3.5 and 0.8 mm. The conversion increased, going from 3.5–2.38 mm to 2.38–2.0 mm, and then remained constant. (c) With the contaminated feed (100 ppm of thiophene) and catalyst A, using the standard experimental conditions and two different particle sizes, 1.41–1.0 and 1.0–0.8 mm. The curves for decay of conversion vs time obtained for both particle sizes were practically coincident. (d) Deactivated catalysts A and C were charged again in the reactor and the reaction was carried out in absence of thiophene, under the standard conditions. In both cases, the conversion was zero. So, these results show that in our experimental conditions, both external and internal diffusional limitations were absent, and a homogeneous distribution of the feed in the reactor was attained.

RESULTS

Characterization

The results of characterization of the catalysts are summarized in Tables 1 to 4 and in Figures 1 to 4.

Catalyst reducibility. TPR profiles of Pd/SiO₂ catalysts, with and without lanthanum promoter, show a single reduction peak, with a maximum that shifts to higher temperatures with increasing amounts of La (see Fig. 1 and Table 1), indicating that La hinders palladium reduction. There are no peaks around 293 K, which indicates the absence of Pd species reduced at room temperature in all the samples. To confirm these results, a 5% H₂ in Ar flow was passed at RT over samples A and C for 24 h, and no reduction was detected. An easily reducible Pd species would be PdO. However, XRD analysis of PdCl₂ calcined at 573 K showed that the only Pd species present was PdCl₂. On the other hand, desorption of hydrogen coming from hydride was not detected, because this species is decomposed at a lower temperature (about 343 K) than that of catalyst reduction in TPR experiments.

The H₂ uptake calculated from the area under the peaks shows that, under the conditions used for catalyst reduction and within the accuracy of the method, palladium is completely reduced (H₂/Pd²⁺ = 1). For the reduction calculations we have assumed a Pd²⁺ oxidation state, which is the state expected for the preparation conditions of our catalysts, according to the literature data (26). Additionally, the presence of Pd⁺ and/or Pd³⁺ can be excluded

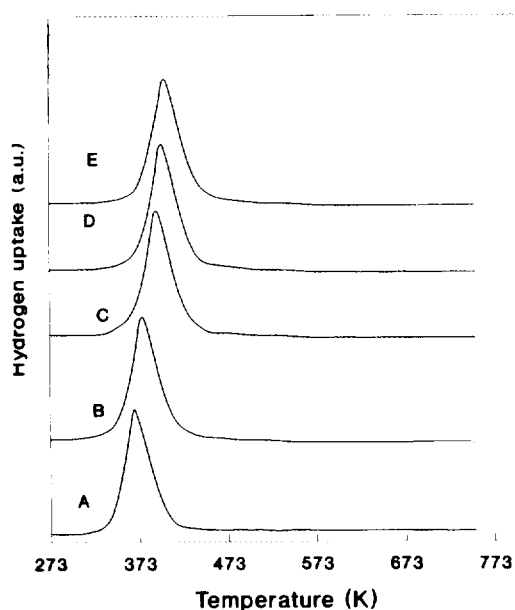


FIG. 1. TPR profiles of the calcined samples.

in our catalysts, from ESR studies of the calcined samples (27). On the other hand, neither bulk nor supported LaCl_3 (sample G) nor La_2O_3 show any H_2 uptake, i.e., they are not reduced between 273 and 973 K. Finally, reduction of La species by H_2 spillover from Pd can be discarded, as will be explained in the next paragraph.

Dispersion. The addition of La produces an increase in Pd dispersion, noticeable for samples B (Pd/La = 1) and C (Pd/La = 2), irrespective of whether the dispersion is measured by CO or H_2 chemisorption (Table 1). The parallel trend in CO and H_2 adsorption with increased La content is in agreement with results reported by Schultz *et al.* (28) for lanthana-promoted Rh/ SiO_2 catalysts, and by Hahm and Lee (29) for Pd catalysts. The parallel increase of the CO/Pd and H/Pd ratios as the La/Pd ratio increases, in addition to the similar dispersion values obtained from both techniques, means that the hydrogen chemisorption increase cannot be attributed to a spillover of H_2 from Pd to La.

X-ray Diffraction. XRD patterns of catalysts show broad peaks corresponding to amorphous silica. The absence of the characteristic reflections of LaCl_3 in our catalysts, even in catalyst E (Fig. 2a), which contains about 5.2 wt% LaCl_3 , cannot be attributed to the low amount of this compound present. We have prepared an additional sample containing 10 wt% $\text{LaCl}_3/\text{SiO}_2$, but without palladium, and it did not exhibit a diffraction pattern (Fig. 2b). These results suggest, therefore, that the LaCl_3 is highly dispersed on the silica surface as an amorphous or microcrystalline phase, analogous to that proposed for the $\text{La}_2\text{O}_3/\text{Al}_2\text{O}_3$ system (30, 31). According to (30) lanthana

is in the form of a two-dimensional overlayer, invisible by XRD up to a concentration of $8.5 \mu\text{mole La m}^{-2}$. Catalyst E has $0.7 \mu\text{mole LaCl}_3 \text{ m}^{-2}$.

We believe that the La species present on our catalysts, at least in a significant concentration, is LaCl_3 . Actually, we have experimentally verified that at the calcination temperature of the catalysts (573 K), the commercial $\text{LaCl}_3 \cdot n\text{H}_2\text{O}$ is not transformed into LaOCl or La_2O_3 (see Fig. 2d). The new lines that appear in this XRD pattern, compared with that of the uncalcined $\text{LaCl}_3 \cdot n\text{H}_2\text{O}$ (Fig. 2c), correspond to partially hydrated LaCl_3 species. LaOCl is only formed after calcination of $\text{LaCl}_3 \cdot \text{aq}$ at 773 K, and La_2O_3 is never formed, not even after calcination at 1073 K, where LaOCl is still the only crystalline phase present (Figs. 2e and 2f). In contrast with the La- Al_2O_3 system, the formation of Si-O-La< species, under the mild thermal treatments given to our catalysts, seems unlikely. Silica has a very stable structure with silanol groups that exhibit some reactivity only at pH > 5. Moreover, the surface concentration of silanol groups is reduced by thermal dehydroxylation above 400 K, being virtually complete at 900 K (32–34). Above 723 K, the formation of siloxane groups is practically an irreversible reaction (35).

However, in order to experimentally confirm that silica is not rehydrated during the impregnation step, the following samples were analyzed by IR spectroscopy: (a) silica calcined at 823 K ($\text{SiO}_2\text{-823}$); (b) $\text{SiO}_2\text{-823}$ impregnated with 1 M HCl aqueous solution; and (c) $\text{SiO}_2\text{-823}$ impreg-

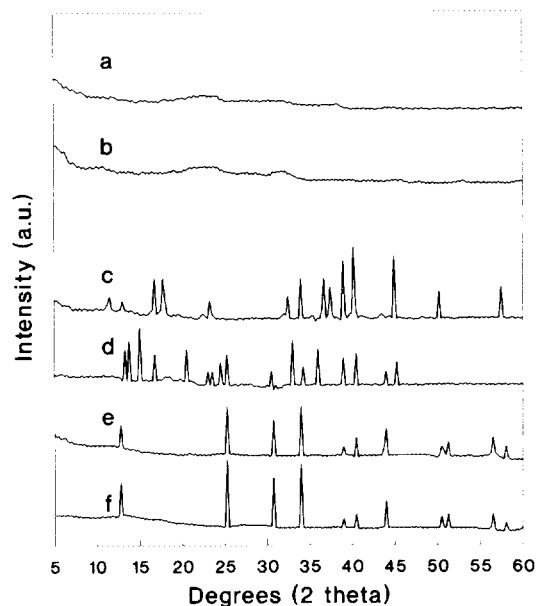


FIG. 2. Diffraction patterns of: (a) catalyst E, (b) 10 wt% $\text{LaCl}_3/\text{SiO}_2$, (c) commercial LaCl_3 , (d) commercial LaCl_3 calcined at 573 K, (e) commercial LaCl_3 calcined at 773 K, and (f) commercial LaCl_3 calcined at 1073 K.

TABLE 2
XPS Data on Catalysts and Standards

Sample	Pd 3d _{5/2}		La 3d _{5/2}	Cl 2p _{3/2}
	BE (eV)	FWHM (eV)	BE (eV)	BE (eV)
Pd (foil)	335.1			
Pd/SiO ₂ ^a	335.2	2.3		—
La ₂ O ₃ ^b			834.6	
LaOCl ^b			834.4	201.1
LaCl ₃ ·7H ₂ O ^b			834.2	201.0
A (0)	336.5	3.5		200.6
B (1)	335.3	2.2	834.0	201.0
C (2)	335.8	2.8	833.2	200.9
D (3)	335.6	2.5	833.6	201.1
E (4.5)	335.3	2.2	833.9	201.0
F (LaCl ₃ /SiO ₂) ^c			834.1	
G (LaCl ₃ /SiO ₂) ^d			834.1	
H (Pd/SiO ₂) ^e	335.0	2.0		
I (PdLa/SiO ₂) ^f	335.1	2.1	834.5	

^a Prepared from PdCl₂. Reduced at 723 K. No Cl 2p_{3/2} peak is detected (40).

^b This work.

^c Uncalcined.

^d Calcined at 573 K.

^e Prepared from Pd(NO₃)₂. Calcined and reduced at 573 K.

^f Prepared from Pd(NO₃)₂ + La(NO₃)₃. (La/Pd = 2.) Calcined and reduced at 573 K.

nated with PdCl₂ or PdCl₂ + LaCl₃. The characteristic silanol bands were never observed.

XPS. Data on the parameters of the XP spectra for the Pd 3d_{5/2}, La 3d_{5/2}, and Cl 2p_{3/2} levels of the fresh catalysts and standards are summarized in Table 2. The binding energy of the Cl 2p_{3/2} peak corresponds to Cl⁻ species, indicating that Cl⁻ ions are not completely removed from the catalysts by the thermal treatments. The O 1s peak at 532.8 eV, corresponding to pure silica, is also observed.

The XPS peaks of the Pd 3d_{5/2} and Pd 3d_{3/2} levels for the catalysts A–D, after smoothing and background subtraction, are given in Fig. 3. The XP spectrum of catalyst E matches that of sample B. As the extent of the BE shifts observed is equal for the two 3d levels, only the BE and FWHM of the Pd 3d_{5/2} level will be used to determine the chemical state of Pd.

The Pd 3d_{5/2} spectrum of catalyst A (La/Pd = 0) consists of a broad peak with a maximum at 336.5 eV and a slight asymmetry towards low binding energies (at about 335.4 eV), suggesting that it is composed of more than one peak. As expected for Pd catalysts prepared from PdCl₂ acid solutions (36), the BE and FWHM values of Pd 3d_{5/2} for this sample (Table 2) indicate the presence of Pd⁰ and electron-deficient Pd species (Pdⁿ⁺). From the shape of the curve, one can conclude that Pdⁿ⁺ is the major species.

The shift in the BE of Pd to a lower value in sample

B, which corresponds to Pd⁰ (Table 2), shows that even in the presence of Cl⁻ ions the incorporation of La decreases the concentration of superficial Pdⁿ⁺. It is noticeable that this effect is produced without modification of the La 3d_{5/2} binding energy, which corresponds to La³⁺. This BE value is closer to that of La in LaCl₃ than in La₂O₃ or LaOCl (see Table 2). Note also that uncalcined and calcined LaCl₃/SiO₂ (samples F and G, respectively) have the same La binding energy. Further addition of La

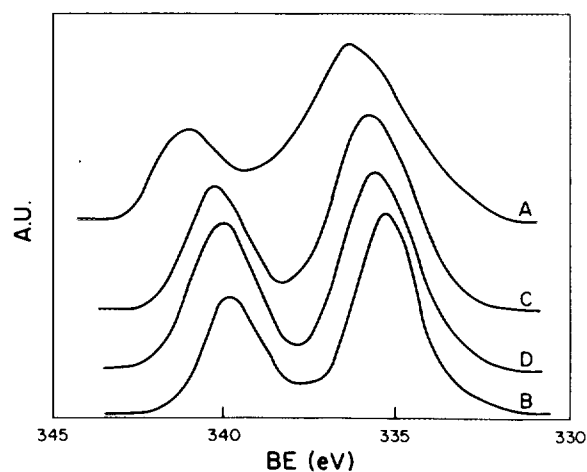


FIG. 3. Pd 3d XPS spectra of fresh catalysts A–D after reduction.

TABLE 3
Atomic Ratio of Species on the Catalysts

Catalyst	La : Pd		La : Si		Pd : Si	
	Bulk ^a	XPS	Bulk ^a	XPS	Bulk ^a	XPS
A	0.0	0.0	0	0	0.0028	0.048
B	1.0	0.9	0.0028	0.04	0.0028	0.042
C	2.0	1.6	0.0056	0.07	0.0028	0.045
D	3.0	2.8	0.0085	0.12	0.0028	0.045
E	4.5	4.3	0.0127	0.17	0.0028	0.042

^a By chemical analysis.

(sample C and possibly sample D) produces a small shift in the BE (less than 1 eV) for both Pd 3d_{5/2} and La 3d_{5/2}, indicating that a weak charge transfer from Pd to La³⁺ or an electron polarization takes place. This transfer is at a maximum for catalyst C (La/Pd = 2), for which the BE of Pd is, nevertheless, lower than that for sample A (La/Pd = 0). These XPS values agree with those obtained by Driessen *et al.* (10), who demonstrated the presence of electron-deficient Pdⁿ⁺ on Pd/SiO₂ catalysts containing lanthana, after acetylacetone extraction. Our results contrast, however, with those reported by Fleisch *et al.* (9), who observed the appearance of a small negative charge on palladium. These differences may probably arise from the different techniques used in catalyst preparation and the different lanthanum species present.

The La/Si and Pd/Si external surface atomic (s) ratios determined by XPS (Table 3), which are higher than the bulk (b) ratios obtained by chemical analysis, indicate that most of the La and Pd is preferentially deposited on the external surface of the support. Likewise, the La_s/La_b ratio is roughly constant (Fig. 4). The parallel increase of La/Pd atomic ratios with La loadings indicates that there is no preferential surface deposition of any of them. On the other hand, the values of the surface Cl/La atomic ratio for all the catalysts, as determined by XPS, are about 3.3.

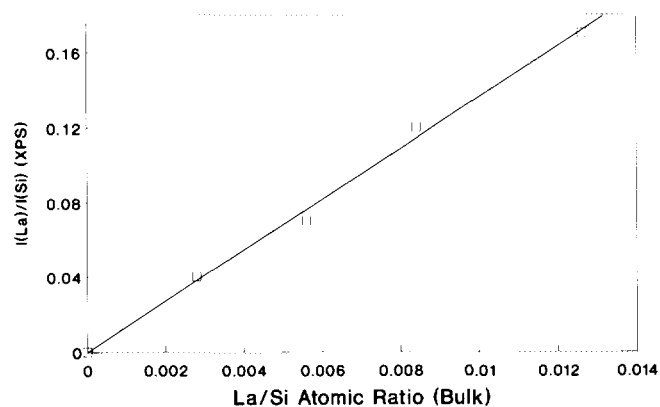


FIG. 4. Relationship between XPS La/Si intensity ratio and La/Si composition atomic ratio.

In order to obtain insight on the chemical state of the catalyst surface after poisoning, XP spectra of deactivated samples were also recorded. These spectra show, in addition to oxidized Pd and Cl⁻ ions, the appearance of a sulfur peak, characteristic of sulfided metal species. The BE and FWHM values for Pd 3d_{5/2}, S 2p, and Cl 2p_{3/2} peaks are given in Table 4. The FWHM of S 2p peaks (about 2.2 eV) suggest that only one sulfur species is present on all the deactivated samples. The number of sulfur atoms per exposed Pd atom ($\theta_E = S/Pd$), obtained from XPS analysis (see Table 5), is roughly constant and close to 1. This value, which was also confirmed by X-ray fluorescence analysis, corresponds to the experimental atomic stoichiometry of a surface palladium sulfide (11, 37).

Catalyst Deactivation

In the absence of poison, we have experimentally verified that all the catalysts exhibit a stable activity, at least for 10 h on stream. In these experiments, ethylcyclohexane was the only detectable product from the hydrogenation of ethylbenzene. Therefore, either coke is not formed or it has no detectable effect. Then, under our experimental conditions, catalyst deactivation in the presence of

TABLE 4
XPS Data of the Deactivated Catalysts

Catalyst	Pd 3d _{5/2}		S 2p		Cl 2p _{3/2}	
	BE (eV)	FWHM (eV)	BE (eV)	FWHM (eV)	BE (eV)	FWHM (eV)
A (0)	336.5	2.4	163.5	2.2	202.2	2.1
B (1)	336.6	2.5	163.4	2.1	202.1	2.2
C (2)	336.6	2.4	163.4	2.2	202.2	2.2
D (3)	336.6	2.5	163.4	2.2	202.2	2.1
E (4.5)	336.6	2.5	163.4	2.2	202.1	2.2

TABLE 5
Hydrogenation Activity and Deactivation
Parameters of the Catalysts

Catalyst	$10^{-19} \times N_{Pd}^a$ (Pd atom)	TOF ^b (min ⁻¹)	SRO ^c	$\theta_{1/2}^c$	$t_{1/2}$ (min)	θ_F^c	θ_E^d
A (0)	1.56	27.4	0.7	0.39	11.6	1.30	1.10
B (1)	1.98	28.3	1.0	0.50	19.4	1.42	0.97
C (2)	2.55	27.0	1.8	0.80	39.0	2.15	1.01
D (3)	3.00	24.4	1.3	0.59	34.0	1.74	1.03
E (4.5)	2.83	26.2	1.1	0.52	28.2	1.56	0.98

^a From CO chemisorption.

^b Molecules of ethylbenzene hydrogenated per exposed Pd atom per minute.

^c Thiophene molecules/Pd atom, from Fig. 5. SRO for $t \rightarrow 0$; $\theta_{1/2}$ for $a = 0.5$; θ_F for $a \approx 0.01$.

^d Number of sulfur atoms per exposed Pd atom in the deactivated samples from XPS analysis.

thiophene is only due to sulfur poisoning. From the conversion values and the dispersions measured by CO chemisorption, the turnover frequencies (TOFs) for fresh catalysts, i.e., the number of molecules of ethylbenzene which reacted per exposed palladium atom per minute, were calculated (see Table 5). These values indicate that the dispersion (11–22%) does not have any appreciable effect on the hydrogenation activity of these catalysts.

In the presence of 100 ppm of thiophene, the conversion decays as a function of time on stream, due to the effect of sulfur, and goes to zero after a given time. This behaviour corresponds to catalysts without thiotolerance (residual activity of the catalyst in the presence of a certain sulfur–compound concentration), although the curves of activity decay for each catalyst show significant differences. The values of the initial TOF (at $t = 0$) are acceptably coincident with those obtained in the absence of thiophene.

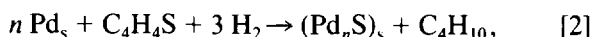
The activity decay is not due to the agglomeration of the palladium particles produced by sulfur. The poisoned samples practically do not chemisorb CO, because the sulfur is strongly bonded to palladium and is not eliminated by thermal treatment at 673 K under a flow of either inert gas or hydrogen. However, when calcined and reduced like the fresh catalysts, these samples practically recover the original dispersion and activity, indicating that most of the sulfur can be removed by air calcination.

In order to compare the stability of the different catalysts on an atomic basis, we have plotted in Fig. 5 the normalized activity as a function of the number of thiophene molecules fed per initially exposed palladium atom, based on CO chemisorption ($\theta =$ thiophene molecules fed/ N_{Pd}); this is a parameter that is proportional to the time on stream. Normalized activity (a) is the ratio between the reaction rate at time t and at time zero (38).

Since the overall sulfur resistance of metal catalysts is a property that depends on: (a) the physicochemical characteristics of the metal atoms and (b) the number of exposed metal atoms, the quantitative comparison of sulfur resistance was done on the basis of both intensive and extensive deactivation parameters (39). These are the *initial catalyst sulfur resistance* (intensive parameter), SRO = the number of thiophene molecules required to deactivate one Pd atom at $t \rightarrow 0$, and the *half-deactivation time* (extensive parameter), i.e., for $a = 0.5$, $t = t_{1/2}$ (see Table 5). SRO is calculated from the slope of the curves at the origin, assuming that the poison is well dispersed on the solid. SRO is a very valuable parameter in the comparison of catalytic stabilities because it is a measure of the refractoriness of the Pd atom to the poison, at low coverage. $t_{1/2}$ is an experimental parameter which can be obtained from the curves by the equation

$$t_{1/2} = \theta_{1/2} (\text{thiophene molecules}/N_{Pd}) \times (N_{Pd}/\text{thiophene molecules min}^{-1}). \quad [1]$$

From the curves in Figure 5, the values of θ_F , number of sulfur atoms fed per atom of exposed palladium necessary to deactivate the catalyst (at normalized activity $a \approx 0.01$), were calculated (see Table 5). Actually, the difference $\theta_F - \theta_E$ is an overall and meaningful measure of the catalyst sulfur resistance, inversely related to the efficiency of the metal poisoning process,



where $n = 1/\theta_E = 1$. The order of the catalyst sulfur resistance given by $\theta_F - \theta_E$ is the same as that obtained

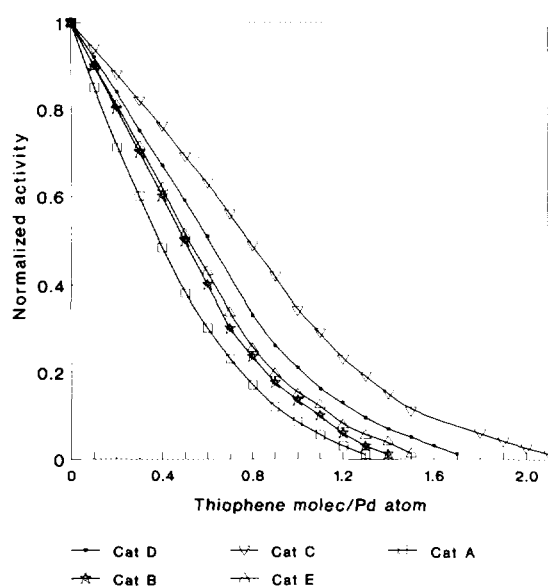


FIG. 5. Deactivation curves of the catalysts by thiophene poisoning.

from SRO and $t_{1/2}$. Comparing the results, it arises that La improves the palladium sulfur resistance, which goes through a maximum for catalyst C (La/Pd = 2), in the range of concentrations studied (Fig. 6). We have demonstrated (40) that a positive correlation exists between the sulfur resistance and the concentration of Pd^{n+} in the surface of the catalyst. In the present case, however, an enhancement of the sulfur resistance of Pd by La^{3+} addition occurs, in spite of an increase in the Pd electronic density. This result proves that lanthanum is able to protect palladium from the toxic effect of thiophene by an alternative mechanism to that leading to the formation of electron-deficient species in the presence of Cl^- . This finding is important because it highlights that it is possible to increase the sulfur resistance of catalysts in which the surface palladium is found in the metallic state (Pd^0). It should be noted that neither $\text{LaCl}_3/\text{SiO}_2$ (sample G) nor $\text{La}_2\text{O}_3/\text{SiO}_2$ showed any catalytic activity in the ethylbenzene hydrogenation.

Furthermore, it must be pointed out that the protective effect of lanthanum does not depend on the presence of Cl^- ions. Actually, a similar result was also observed with a chlorine-free catalyst prepared just for comparative purposes. A Pd/SiO_2 catalyst (sample H) was prepared starting from $\text{Pd}(\text{NO}_3)_2$ and another (sample I, La/Pd = 2) was prepared by coimpregnation with $\text{Pd}(\text{NO}_3)_2$ and $\text{La}(\text{NO}_3)_3$. Both were calcined and then reduced at 573 K. The effect of the different species on the sulfur resistance is presented in Table 6. SRO_r is the initial sulfur resistance of catalysts relative to that of sample H. It

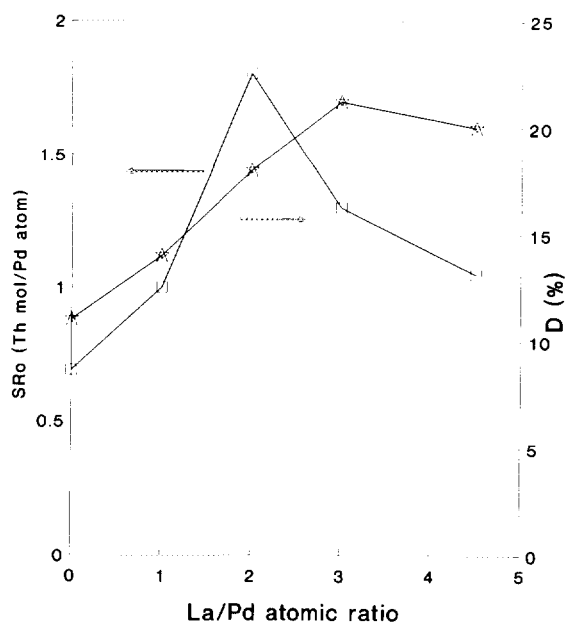


FIG. 6. Effect of lanthanum content on the sulfur resistance and palladium dispersion.

TABLE 6
Effect of Various Species on the Sulfur Resistance of the Catalysts

Catalyst	H	A	I	B	E	D	C
Precursor	N	Cl	N	Cl	Cl	Cl	Cl
La/Pd	0	0	2	1	4.5	3	2
Pd^{n+}	NO	HIGH	NO	NO	NO	(?)	MEDIUM
SRO_r	1	4.3	5.0	6.3	6.6	7.7	10.8

Note. Precursors: N = Nitrates; Cl = Chlorides. SRO_r : SRO relative to SRO of the sample H.

was found (40) that palladium in catalysts prepared from $\text{Pd}(\text{NO}_3)_2$ is zerovalent (BE 335.0 eV) and deactivates faster than in catalysts containing Cl^- and Pd^{n+} . This can now be observed by comparing catalysts H and A (see Tables 2 and 6). The presence of La (in this case as La_2O_3 , sample I) does not modify the BE of $\text{Pd } 3d_{5/2}$ (Pd^0) (Table 2) but it produces a remarkable enhancement in Pd sulfur resistance, even more than that produced by electron-deficient Pd in the presence of chlorine species (compare samples A and I, Table 6). It is noticeable that when both lanthanum and Pd^{n+} species are present, the resistance of Pd to thiophene is even higher.

DISCUSSION

It is generally accepted that the mechanism of metal poisoning by thiophene at temperatures above 423 K involves the strong chemisorption of the sulfur compound on the metal sites followed by its hydrogenolysis, leading to a stable and inactive metal-sulfur species on the surface (11, 41). In fact, butane but not hydrogen sulfide was detected in our experiments, and XPS analysis showed the formation of metal sulfide species on the spent catalysts (Table 4).

The hydrogenolysis of thiophene, similar to that of hydrocarbons, is a structure-sensitive reaction (42) which requires relatively large ensembles of adjacent metal atoms to enable the multiple anchoring of the molecule, a prerequisite for breaking the C-S bond. In addition, the higher the electron-donor character of the metal site the stronger the metal-sulfur bond and the easier the sulfur compound hydrogenolysis (43).

The increase in the H_2 and CO chemisorption on palladium with increased La/Pd ratio, along with the fact that neither La_2O_3 nor LaOCl are observed on the catalysts, indicates that an explanation of the effect of lanthanum based on the decoration of the reduced palladium particles by La species, analogous in nature to that described elsewhere (7), is very improbable. This conclusion is in agreement with results obtained by Schultz *et al.* for Rh-La/ SiO_2 (28).

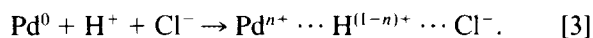
On the other hand, the modification of sulfur resistance by lanthanum does not appear to be caused by the change in palladium dispersion (Fig. 6). Actually, the influence of dispersion on the sulfur resistance of metal catalysts is not clear-cut in the literature (44–47). Recently, it was reported that the metal dispersion has no effect on the sulfur resistance of Ni catalysts in benzene hydrogenation (48) or of Pd catalysts in cyclohexane dehydrogenation (49), in the presence of thiophene.

Within the narrow dispersion range of our catalysts, no evident relationship is found between stability and dispersion. In fact, in most cases, the initial sulfur resistance of catalysts and their lifetime increase more than linearly with the number of exposed Pd atoms, as can be deduced from Table 5 and Fig. 6. For example, catalyst C has 1.6 times more exposed Pd atoms than catalyst A but it is initially about 2.6 times more resistant, and its half deactivation time is about 3.5 times higher. Similar conclusions can be drawn if one compares the other catalysts. In particular, catalyst C is more sulfur resistant than catalysts D or E in spite of its lower dispersion. Therefore, although from our results we cannot discard that crystal size may have some influence on sulfur resistance, it appears that the role of La is not merely limited to increasing the metal dispersion.

Another possible explanation of the effect of lanthanum, can also be discarded, based on the adsorption of sulfur by La species. If La acts as a sulfur acceptor, the amount of sulfur in the spent catalysts would increase with La concentration, which obviously is not the case, as is shown in Table 5. The S/Pd experimental atomic ratio of the deactivated catalysts (θ_E) is constant and independent of the La/Pd atomic ratio. In addition, on the basis of this hypothesis, the values of the sulfur resistance of the catalysts would be inconsistent.

Therefore, we think that La³⁺ can play a mainly geometric role. This hypothesis may reasonably account for the more outstanding findings of this work, namely, (a) the unexpected decrease of the Pd BE in catalysts prepared from H₂PdCl₄ and (b) the parallel increase in sulfur resistance.

(a) In the surface of catalysts prepared from PdCl₂ acid solutions (even after careful reduction below 723 K), due to the high palladium–hydrogen bond strength (50), Pdⁿ⁺ species would be formed by the interaction of Pd⁰ with neighbouring H⁺, originated during the reduction step, through bridge structures stabilized by the Cl⁻ ions (14).



Accordingly, electron-deficient Pdⁿ⁺, present in our reduced catalyst A, is not unreduced Pd²⁺ but Pd⁰ sharing the positive charge of the proton. Actually, PdCl₂ is completely reduced at 573 K, as our TPR results show. So,

the amount of Pdⁿ⁺ formed depends on the amount of remaining adsorbed HCl, which is a function of the reduction temperature (14, 40). Thus, when PdCl₂/SiO₂ is reduced at 723 K, all HCl is removed (40) and electron-deficient palladium is not formed (Table 2). In some ways, this mechanism is similar to that proposed by Homeyer *et al.* (51) and Sachtler and Stakheev (50) to explain the presence of electron-deficient palladium in chloride-free Pd/Y zeolite reduced catalysts.

In the solutions used to prepare the catalysts, Pd and La precursors are homogeneously mixed, in such a way that they are uniformly dispersed on the support in the impregnation step. After drying, La³⁺ is located in close proximity to Pd²⁺ (29, 52), hindering the interaction Pd⁰ ⋯ H⁺ and preventing the formation of Pdⁿ⁺. This would explain the shift of the BE of Pd 3d_{5/2} to a lower value, observed upon the incorporation of La. TPR, XPS, and dispersion results, which clearly show that a certain Pd–La³⁺ interaction exists, consistently support this statement.

The BE values for Pd and La show that on certain catalysts, however, a slight electron density transfer Pd → La takes place, with a maximum for catalyst C (La/Pd = 2). This is a very surprising result, considering the practical irreducibility of the La³⁺, under the conditions used in this work, as TPR and the literature data confirm (2, 3, 53). However, taking into account the low lanthanum loadings of our catalysts (La/Si ≤ 0.01 atom/atom) and the XPS and XRD results, one can assume that most of the lanthanum is highly dispersed on the surface. Furthermore, the Lewis acid character of deficiently coordinated high valence cations (such as La³⁺ and Fe³⁺) existing on the surface of the supports, is well documented in the literature (31, 54, 55). In such a case, it can be assumed that, although La exists as irreducible La³⁺ in the bulk, probably due to a decrease in the repulsive Madelung potential at the La sites (31, 56, 57), surface La³⁺ cations could be partially reduced through a local electron coordinative interaction with the nearest electron-donor Pd⁰ species, as was reported for similar cases (56). The binding energy of Pd 3d_{5/2} in catalyst C, however, is lower than that of Pd in a catalyst without La (sample A), probably due to the fact that the polarization Pd⁰ → La³⁺ is more difficult than Pd⁰ → H⁺.

(b) In this model, due to the vicinity of Pd–La³⁺ on the surface, inactive LaCl₃ would play a diluent role, disrupting the Pd⁰ ensembles and restricting the multisite adsorption of thiophene and its subsequent hydrogenolysis. Similar geometrical hypotheses were also suggested to explain the effect of other ionic species on the catalytic properties of metals (52, 58). As the ethylbenzene hydrogenation is rather a structure-insensitive reaction (42), the hydrogenation activity is less affected by the presence of lanthanum (see the TOFs in Table 5). As a consequence,

catalysts containing La are more sulfur resistant than catalyst A itself, in spite of the fact that the latter has a higher concentration of electron-deficient palladium (Pd^{n+}).

Although this geometric effect of lanthanum accounts for the observed increase in sulfur resistance, our experimental results indicate that an electronic effect is also operative. As the thiophene adsorption strength on the Pd^{n+} species is lower than on Pd^0 , one might reasonably expect that the rupture of the C–S bond would be inhibited when surface La^{3+} and Pd^{n+} species are present (42). Thus, catalyst C, which exhibits the highest sulfur resistance, also has Pd^{n+} species, which cooperate with the geometrical effect produced by La^{3+} .

A maximum of the catalytic effect for a given promoter cation concentration has been frequently observed (2, 10, 59, 60). For La–Pd system, Choudary *et al.* (8) observe a maximum of activity in methanol synthesis for an atomic La/Pd ratio of 0.7. The reason for the existence of these maxima, however, is not yet entirely clear. Indeed, if one accepts that the interaction Pd–La is localized in the Pd– LaCl_3 interface (2), then one can expect that this interaction, and therefore the sulfur resistance, goes through a maximum (sample C), because the size of the interface also goes through a maximum. For catalysts with La/Pd > 2, the sulfur resistance decreases, probably due to the fact that in such a case aggregates of LaCl_3 can be deposited and the size of the interface will decrease. Consequently, the geometric effect of La^{3+} on Pd ensembles and electron transfer does not occur or it is produced in a lower extent.

CONCLUSIONS

The results obtained in this work show that the addition of LaCl_3 to a Pd/ SiO_2 catalyst increases the reduction temperature and dispersion of palladium and modifies its electronic state. Additionally, lanthanum improves the resistance of the catalysts to thiophene poisoning in ethylbenzene hydrogenation, in spite of the fact that it reduces the concentration of electron-deficient Pd species. The enhancement of the sulfur resistance of the catalyst with lanthanum is not produced by the decoration of palladium by La or by the adsorption of sulfur by La species. Neither it can be simply related to the increase in Pd dispersion. According to our results, La and Pd are deposited preferentially on the external surface. Lanthanum is present as very well dispersed LaCl_3 , in close vicinity to palladium crystallites. It is possible therefore that lanthanum essentially plays a geometric role, disrupting the Pd^0 ensembles required for the multianchoring and subsequent hydrogenolysis of the thiophene molecule, which is a step prior to the catalyst poisoning. At certain La/Pd ratios there also exists an electronic effect which generates Pd^{n+} species, which are more sulfur resistant than Pd^0 . This effect is at

a maximum for the sample with La/Pd = 2 and, therefore, this catalyst exhibits the higher sulfur resistance. For catalysts with La/Pd > 2, sulfur resistance decreases, probably because LaCl_3 aggregates can be formed and the size of the Pd– La^{3+} interface decreases.

ACKNOWLEDGMENTS

Financial support from CICYT, Spain (Project MAT90-0808), CONICET, Argentina (Project ID 640), and the Programa de Cooperación Científica con Iberoamérica of the MEC (ICI-AECI), Spain, is gratefully acknowledged.

REFERENCES

1. Karpinski, Z., *Adv. Catal.* **37**, 45 (1990).
2. Borer, A. L., and Prins, R., in "Proceedings, 10th International Congress on Catalysis, Budapest, 1992" (L. Guzzi, F. Solymosi, and P. Tétényi, Eds.), Vol A, p. 765. Akadémiai Kiadó, Budapest, 1993.
3. Kieffer, R., Kiennemann, A., Rodriguez, M., Bernal, S., and Rodriguez-Izquierdo, J. M., *Appl. Catal.* **42**, 77 (1988).
4. Hicks, R. F., and Bell, A. T., *J. Catal.* **90**, 205 (1984).
5. Sudhakar, Ch., and Vannice, M. A., *J. Catal.* **95**, 227 (1985).
6. Nogin, Yu. N., Chesnokov, N. V., and Kovalchuk, V. I., *Catal. Lett.* **23**, 79 (1994).
7. Rieck, J. S., and Bell, A. T., *J. Catal.* **96**, 88 (1985).
8. Choudary, B. M., Matusek, K., Bogyay, I., and Guzy, L., *J. Catal.* **122**, 320 (1990).
9. Fleisch, T. H., Hicks, R. F., and Bell, A. T., *J. Catal.* **87**, 398 (1984).
10. Driessen, J. M., Poels, E. K., Hindermann, J. P., and Ponc, V., *J. Catal.* **82**, 26 (1983).
11. Boitiaux, J. P., Cosyns, J., and Verna, F., *Stud. Surf. Sci. Catal.* **34**, 105 (1987).
12. Bartholomew, C. H., Agrawal, P. K., and Katzer, J. R., *Adv. Catal.* **31**, 135 (1982).
13. Barbier, J., Lamy-Pitara, E., Marecot, P., Boitiaux, J. P., Cosyns, J., and Verna, F., *Adv. Catal.* **37**, 279 (1990).
14. Seoane, X. L., L'Argentiere, P. C., Fígoli, N. S., and Arcoya, A., *Catal. Lett.* **16**, 137 (1992).
15. Boudart, M., and Hwang, H. S., *J. Catal.* **39**, 44 (1975).
16. Martín, M. A., Pajares, J. A., and González-Tejuca, L., *J. Colloid Interface Sci.* **107**, 540 (1985).
17. Farrauto, J. R., *AIChE Symp. Ser.*, **70**, p. 143, 1974.
18. Ott, G. L., Fleisch, T. H., and Delgass, W. N., *J. Catal.* **60**, 394 (1979).
19. Scofield, J. H., *J. Electron Spectrosc. Relat. Phenom.* **8**, 129 (1976).
20. Prada Silvy, R., Beuken, J. M., Fierro, J. L. G., Bertrand, P., and Delmon, B., *Surf. Interface Anal.* **8**, 167 (1986).
21. Shyu, J. Z., Otto, K., Watkins, W. L., Graham, G. W., Belitz, R. K., and Gandhi, H. S., *J. Catal.* **114**, 23 (1988).
22. Noak, K., and Zbinden, H., *Catal. Lett.* **4**, 145 (1990).
23. Pitchon, V., Guenin, M., and Praliaud, H., *Appl. Catal.* **63**, 333 (1990).
24. Seoane, X. L., Arcoya, A., González, J. A., and Travieso, N., *Ind. Eng. Chem. Res.* **28**, 260 (1989).
25. Levenspiel, O., "Chemical Reaction Engineering," Chap. 14. Wiley, New York, 1966.
26. Bozon-Verduraz, F., Omar, A., Escard, J., and Pontvianne, B. J., *J. Catal.* **53**, 126 (1978).
27. Arcoya, A., Fígoli, N. S., L'Argentiere, P. C., Seoane, X. L., and Soria, J., unpublished results.

28. Schultz, E., Borer, A. L., and Prins, R., *Catal. Lett.* **14**, 279 (1992).
29. Hahm, H. S., and Lee, W. Y., *Appl. Catal.* **65**, 1 (1990).
30. Bettman, M., Chase, R. E., Otto, K., and Weber, W. H., *J. Catal.* **117**, 447 (1989).
31. Odriozola, J. A., Carrizosa, I., and Alvero, R., *Stud. Surf. Sci. Catal.* **48**, 713 (1989).
32. Shyu, J. Z., Goodwin, J. G., Jr., and Hercules, D. M., *J. Phys. Chem.* **89**, 4983 (1985).
33. Wu, M., and Hercules, D. M., *J. Phys. Chem.* **83**, 2003 (1979).
34. Acres, G. J. H., Bird, A. J., Jenkins, J. W., and King, F., in "Catalysis," Vol. 4, Chap. 1. Royal Society of Chemistry, London, 1980.
35. Winyall, M. E., in "Applied Industrial Catalysis," (Bruce E. Leads, Ed.), Vol. 3, p. 55. Academic Press, New York, 1984.
36. L'Argentiere, P. C., Figoli, N. S., Arcoya, A., and Seoane, X. L., *React. Kinet. Catal. Lett.* **43**(2), 413 (1991).
37. Arcoya, A., Cortés, A., Fierro, J. L. G., and Seoane, X. L., *Stud. Surf. Sci. Catal.* **68**, 557 (1991).
38. Ereckson, E. J., and Bartholomew, C. H., *Appl. Catal.* **5**, 323 (1983).
39. Bartholomew, C. H., and Uken, A. H., *Appl. Catal.* **4**, 19 (1982).
40. Arcoya, A., Seoane, X. L., Figoli, N. S., and L'Argentiere, P. C., *Appl. Catal.* **62**, 35 (1990).
41. Bourne, K. H., Holmes, P. D., and Pitkethly, R. C., in "Proceedings, 3rd International Congress on Catalysis, Amsterdam, 1964," Vol. II, p. 1401. North-Holland, Amsterdam, 1965.
42. Sinfelt, J. H., in "Chemistry & Physics of Solids Surfaces" (R. Vanselow and R. Howe, Eds.), Vol. 6, p. 19. Springer-Verlag, Berlin, 1986.
43. Biswas, J., Bickle, G. M., Gray, P. G., and Do, D. D., *Stud. Surf. Sci. Catal.* **34**, 553 (1987).
44. Rabo, J. A., Schomaker, V., and Pickert, P. E., in "Proceedings, 3rd International Congress on Catalysis, Amsterdam, 1964," Vol. II, p. 1264. North-Holland, Amsterdam, 1965.
45. Echevski, G. V., and Ione, K. G., *Stud. Surf. Sci. Catal.* **5**, 273 (1980).
46. Duprez, D., and Mendez, M., *Stud. Surf. Sci. Catal.* **34**, 523 (1987).
47. Guenin, M., Breyse, M., Frety, R., Tifouti, K., Marecot, P., and Barbier, J., *J. Catal.* **105**, 144 (1987).
48. Marecot, P., Paraiso, E., Daumas, J. M., and Barbier, J., *Appl. Catal.* **80**, 79 (1992).
49. Hoyos, L. J., Primet, M., and Praliaud, H., *J. Chem. Soc. Faraday Trans.* **88**, 113 (1992).
50. Sachtler, W. M. H., and Stakheev, A. Yu., *Catal. Today* **12**, 283 (1992).
51. Homeyer, T., Karpinski, Z., and Sachtler, W. M. H., *J. Catal.* **123**, 60 (1990).
52. Schwank, J., Balakrishnan, K., and Sachdev, A., in "Proceedings, 10th International Congress on Catalysis, Budapest, 1992" (L. Guzzi, F. Solymosi, and P. Tétényi, Eds.), Vol. A, p. 905. Akadémiai Kiadó, Budapest, 1993.
53. Shelef, M., Haack, L. P., Soltis, R. E., de Vries, J. E., and Logothetis, E. M., *J. Catal.* **137**, 114 (1992).
54. Connell, G., and Dumesic, J. A., *J. Catal.* **105**, 285 (1987).
55. Haack, L. P., de Vries, J. E., Otto, K., and Chattha, M. S., *Appl. Catal. A Gen.* **82**, 199 (1992).
56. Wolfram, T., and Ellialtioglu, S., in "Theory of Chemisorption" (J. R. Smith, Ed.), Chap. 6. Springer-Verlag, Berlin, 1980.
57. Coix, P. A., "The Electronic Structure and Chemistry of Solids," Chap. 7.6. Oxford Univ. Press, New York, 1987.
58. Martinez Correa, J. A. M., de Miguel, S. R., Baronetti, G. T., Castro, A. A., and Scelza, O. A., in "Proceedings, 10th International Congress on Catalysis, Budapest, 1992" (L. Guzzi, F. Solymosi, and P. Tétényi, Eds.), Vol. C, p. 2211. Akadémiai Kiadó, Budapest, 1993.
59. Underwood, R. P., and Bell, A. T., *J. Catal.* **111**, 325 (1988).
60. Marinelli, T. B. L. W., Vleeming, J. H., and Ponc, V., in "Proceedings, 10th International Congress on Catalysis, Budapest, 1992" (L. Guzzi, F. Solymosi, and P. Tétényi, Eds.), Vol. B, p. 1211. Akadémiai Kiadó, Budapest, 1993.